Pu.1/Spi1 dosage controls the turnover and maintenance of microglia in zebrafish and mammals

Yi Wu[1#], Weilin Guo[2#], Haoyue Kuang[3], Xiaohai Wu[3] , Yuexin Wang[3], Shizheng Zhao[1], Tao Yu[1,3*]

[1]Shenzhen Key Laboratory for Neuronal Structural Biology, Biomedical Research Institute, Shenzhen Peking University-the Hong Kong University of Science and Technology Medical Center, Shenzhen 518036, China;

[2]Research and Development Center, Yaneng BIOscience (Shenzhen) Co Ltd, Shenzhen, Guangdong, China.

[3]Greater Bay Biomedical Innocenter, Shenzhen Bay Laboratory, Shenzhen 518055, China;

[#]These authors contribute equally to this work.

Correspondence should be addressed to: tyu@connect.ust.hk

Abstract

Microglia are brain-resident macrophages that play pivotal roles in CNS development and homeostasis. Yet, the cellular and molecular basis governing microglia maintenance remain largely unknown. By using a visible conditional knockout strategy to generate mosaic zebrafish, we show that microglia deficient for Pu.1/Spi1b, the master regulator for microglia development, are less competitive and chronically eliminated in a Tp53-dependent manner. Interestingly, when both Pu.1 and Spi-b (the paralogue of Pu.1 in zebrafish, also called Spi1a) are defective, microglia are rapidly depleted via apoptosis, suggesting that Pu.1 and Spi-b regulate the maintenance of microglia in a dosage-dependent manner. More importantly, the dosage dependent regulation of microglia maintenance by Pu.1/Spi1 is also evolutionarily conserved in mouse, as revealed by conditional knockout of *Pu.1* by 1 or 2 alleles in microglia respectively. Collectively, our data pinpoints the conserved cellular and molecular mechanisms controlling microglia turnover and maintenance in teleost and mammals.

Introduction

Microglia, the crucial immune cells residing in the central nervous system (CNS), have a profound impact on the maintenance of CNS homeostasis, as they not only function as scavengers to facilitate the removal of invading pathogens or damaged tissues, but also actively regulate neurogenesis, synaptic pruning and neuronal activity (Colonna and Butovsky, 2017; Gomez-Nicola and Perry, 2015). It is therefore not surprising that the dysfunction of microglia is closely linked with the occurrence and progression of many neurodegenerative disorders (Glass et al., 2010; Li et al., 2012; Prinz et al., 2011), thus making it a promising therapeutic target in the prevention and treatment of these diseases.

In mice, fate-mapping methods revealed that unlike other glia cells with neuroectoderm origin, microglia in adult originate from yolk-sac (YS) derived primitive macrophages, which colonize the developing brain rudiment during early embryogenesis (Ginhoux et al., 2010; Schulz et al., 2012). Whether microglia in adult mammals were contributed by monocyte-derived microglia precursors had long been a debate until the establishment of parabiosis assay (Ajami et al., 2007). It is now well-accepted that under physiological condition microglia in mice are maintained locally by self-renewal throughout the lifespan. In accordance with this concept, microglia population was found to be rapidly reconstituted by resident cells after genetic or pharmacological ablation of microglia (Bruttger et al., 2015; Elmore et al., 2014). However, when estimating the physiological turnover rate of microglia via different methods such as ^{3}H-thymidine/BrdU/EdU incorporation, Ki67 staining or two photon live imaging, different studies yielded distinct or even contradictory results i.e., the estimated microglia turnover rate ranging from 0.13 to 0.8% (Askew et al., 2017; Füger et al., 2017; Lawson et al., 1992; Tay et al., 2017), which indicated that microglia in adult mice (~2 years lifespan) were either long-lived without replenishment or replenished for several times during the whole lifespan of the animals. Nonetheless, these studies have reached the consensus that in adult mice all microglia have the proliferation capability and there are no putative microglia precursors existing to proliferate asymmetrically and continuously to contribute to microglia pool. Moreover, microglia proliferation had been shown to be spatially and temporally coupled with apoptosis to maintain the homeostasis of their population (Askew et al., 2017): which indicates that not only proliferating microglia locate near the dying microglia, but also newborn microglia manifest a higher frequency of apoptosis. However, whether this phenomenon is for the quality control of microglia or has any other physiological relevance remained unclear. In addition, as a fraction of newborn microglia underwent apoptosis and did not contribute to microglia homeostasis, previously calculated proliferation rate might potentially over-estimate the true turnover rate of microglia. Collectively, although these studies give some insights into the understanding of microglia turnover and maintenance, our knowledge about the underlying cellular and molecular mechanisms are still limited.

PU.1, the E-twenty six (ETS) family transcription factor, is one of the best-characterized gene governing the development of macrophage lineage (McKercher et al., 1996; Scott et al., 1994). Disruption of PU.1 in mice causes early lethality of the embryos and complete absence of macrophages (McKercher et al., 1996; Scott et al., 1994), including microglia in brain (Kierdorf et al., 2013). Interestingly, the *PU.1* expression level was found to remain at a high level in microglia after their terminal differentiation (Walton et al., 2000), implying that PU.1 also regulates the cellular behaviors and functions of microglia in the sophisticated CNS environment. Indeed, Chromatin immunoprecipitation (ChIP)-Seq analysis with microglia cell line BV2 cells revealed thousands of PU.1 targets (Satoh et al., 2014). Accordingly, silencing of PU.1 by siRNA in mixed human glial culture led to the reduced viability of microglia and decreased phagocytosis of amyloid-beta (Aβ42) (Smith et al., 2013). However, whether PU.1 indeed regulated the survival and maintenance of microglia in the in-vivo conditions remained to be further investigated, as a previous study reported that inactivating either 1 copy or 2 copies of PU.1 by fusing PU.1 with cytoplasm-retaining estrogen receptor (ER) had no effect on the viability of alveolar macrophages (Karpurapu et al., 2011). Moreover, human SNPs that altered *PU.1* expression level were reported to be associated with Alzheimer's disease (AD) pathogenesis (Cao et al., 2022; Huang et al., 2017). A recent study showed that conditional inactivation or pharmacological inhibition of PU.1 in AD mouse model ameliorated neuroinflammation, prevented microgliosis and improved cognitive performance (Ralvenius et al., 2023). Although reduction of microglia number was considered as a result of the amelioration of neuroinflammation, whether PU.1 directly regulated microglia survival and maintenance to prevent the propagation of neuroinflammation in diseased condition deserved to be carefully revisited.

Owing to the genetic amenability and the feasibility for live-imaging and lineage tracing, zebrafish has been adopted as an ideal model for the study of microglia development and function. Zebrafish microglia are highly conserved with their mammalian counterparts in terms of morphology, molecular signatures, development-regulatory genetic networks as well as functions (Li et al., 2012; Peri and Nüsslein-Volhard, 2008; Xu et al., 2015; Yu et al., 2017). Different from the single origin of mouse microglia, zebrafish microglia were shown to arise from two distinct sources i.e., the rostral blood (RBI), equivalent of mouse YS for primitive myelopoiesis, and the aorta-gonad-mesonephros (AGM) region for hematopoietic stem cell (HSC) initiation. The RBI microglia colonize the developing brain during early embryogenesis, but are gradually replenished by AGM adult microglia (Xu et al., 2015). Further study revealed that this dynamic shift of microglia pool is controlled by Il34-Csf1ra signaling-dictated cell competition (Yu et al., 2023). Yet, when the microglia pool is established in adult zebrafish, the molecular mechanisms underlying their turnover and maintenance remain incompletely understood. Moreover, although Pu.1 and its paralogue Spi-b, the zebrafish orthologues of mammalian PU.1 and SPI-B, were shown to be indispensable for microglia early

development of both origins in zebrafish (Xu et al., 2015; Yu et al., 2017), their functions in the survival and maintenance of microglia in adult animals have not been established.

In the present study, via the condition knockout strategy to generate mosaic microglia population in adult zebrafish and mice, we revealed that the maintenance of microglia is evolutionarily conserved and regulated by Pu.1/Spi1 dosage from teleost to mammals.

Results

Characterization of microglia turnover in adult zebrafish brain

Previous studies have shown that there are two major subtypes of myeloid cells, i.e., *ccl34b.1*$^{+}$ microglia and *ccl34b.1*$^{-}$*ccl19a.1*$^{+}$ brain-resident dendritic cells (DCs) in adult zebrafish brain (Wu et al., 2020; Zhou et al., 2023). To monitor the turnover and maintenance of microglia in adult zebrafish brain, we employed microglia-specific *TgBAC(ccl34b.1:eGFP)* transgenic reporter line (Wu et al., 2020) and performed EdU pulse-chase experiment. We intraperitoneally injected EdU into adult *TgBAC(ccl34b.1:eGFP)* fish for either 1, 3 or 5 consecutive days and then collected the fish brain at 1 day post injection (dpi) for cryosection and GFP/Lcp1/EdU/DAPI co-staining, in which ccl34b.1-GFP^{+} cells are microglia and ccl34b.1-GFP^{-}Lcp1^{+} cells represent DCs (Fig. 1A). Quantification results showed that, while a single dose of EdU pulse labeled 1.892±0.234% microglia, the EdU incorporate rate for microglia after 3 or 5 doses of EdU pulses increased almost linearly (Fig. 1B, green bars). Based on these data, the estimated microglia turnover rate (daily) is ~2.6% (total EdU incorporation rate divided by the times of EdU-pulses) (Fig. 1C, green bars). On the other hand, the EdU incorporate rate for the DCs was much lower (Fig. 1B-C, red bars), suggesting that the DCs in the brain are relatively steady with a very low turnover rate.

To clarify whether there might be putative microglial precursors that continuously proliferate to contribute to microglia turnover, we employed the EdU/BrdU dual-pulse strategy, in which adult WT fish were injected with a single dose of EdU followed with five daily BrdU pulses to determine the BrdU proliferation rate of EdU^{+} and EdU^{-} microglia (Fig. 1D, upper panel). Quantification result showed that the BrdU incorporation rates were comparable between EdU^{+} and EdU^{-} microglia pools (Fig. 1D-E). These data strongly suggest that, similar to mammals (Tay et al., 2017), microglia in adult zebrafish randomly undergo proliferation and there are no well-defined microglial precursors that continuously proliferate to replenish and maintain the microglia pool.

Generation and characterization of the visible conditional knockout allele *pu.1*^{KI}

To elucidate the molecular mechanisms underlying microglia turnover and maintenance, we focused on the Ets family transcription factor PU.1/SPI1, which had been shown to be a master regulator for macrophage/microglia development in fish and mammals (McKercher et al., 1996; Scott et al., 1994;

Yu et al., 2017). Because macrophages/microglia development is completely blocked at early development in *pu.1*-null zebrafish mutants (Yu et al., 2017), we decided to generate a visible *pu.1* conditional knockout allele $pu.1^{KI}$ to study the role of Pu.1 in microglia maintenance via the Non-homologous end jointing (NHEJ)-mediated knock-in method (Fig. 2A and Fig. S1A) (Li et al., 2015). As shown in Fig. 2A, the knock-in DNA fragment consisted of loxP, *pu.1* exon 4 to 6 followed by the self-cleaving P2A sequence-conjugated eGFP, and a splicing-acceptor site SpA2 followed by the P2A-DsRed. In addition, the 3' downstream sequence of *pu.1* gene (gray box) was added to the 3' end of each fluorescent protein to ensure efficient termination of RNA transcription and proper expression of the fluorescent proteins.

Three different founders were obtained. PCR and deep sequencing analysis of F1 embryos confirmed the correct integration of donor DNA fragment in the *pu.1* locus (Fig. S1B-C). Since the knock-in $pu.1^{KI}$ allele would generate intact Pu.1 and eGFP concurrently (Fig. 2A), we predicted the expression pattern of eGFP, which presumably represents the expression of the knock-in Pu.1, should completely overlap with the endogenous Pu.1. Indeed, co-staining of eGFP and Pu.1 antibodies revealed a perfect overlap of the $eGFP^{+}$ cells and $Pu.1^{+}$ cells in $pu.1^{KI/+}$ embryos (Fig. 2B), suggesting that the $pu.1^{KI}$ allele recapitulates the expression of endogenous *pu.1*. This conclusion was further supported by the co-localization of DsRed and eGFP signals in the brains of 3 dpf $pu.1^{KI/+}$*;Tg(mpeg1:LRLG)* embryos and by the co-staining of eGFP and Lcp1 antibodies on the brain sections of adult $pu.1^{KI/+}$ fish (Fig. 2C and D). To further confirm functional intactness of the $pu.1^{KI}$ allele, we crossed the $pu.1^{KI}$ fish with the $pu.1^{\Delta 839}$ mutants to examine if the $pu.1^{KI}$ allele is capable of rescuing the microglia phenotype. Indeed, quantification of microglia number revealed no difference between the $pu.1^{\Delta 839/KI}$ and $pu.1^{\Delta 839/+}$ embryos (Fig. 2E and F), indicating that the $pu.1^{KI}$ allele functionally recapitulates the endogenous *pu.1*.

To test whether the Cre mediated excision occurs correctly in the $pu.1^{KI}$ allele, we injected Cre mRNA into the $pu.1^{KI}$ embryos at one-cell stage. The injected embryos were raised to adulthood ($pu.1^{CKO}$ fish) and crossed with the $pu.1^{KI}$ fish to generate $pu.1^{CKO/KI}$ fish. As illustrated in Fig. 2A, the Cre-mediated excision should remove the E4-6-P2A-eGFP cassette and allow the proper splicing of the splicing-acceptor site SpA2 and joining of the P2A-DsRed with exon 3 (Fig. 2A), leading to the induction of DsRed expression. Indeed, fluorescent imaging of the $pu.1^{CKO/KI}$ embryos revealed robust DsRed ($pu.1^{CKO}$ allele) signals perfectly overlapping with the eGFP ($pu.1^{KI}$ allele) signals (Fig 2G), suggesting the correct DNA excision and RNA splicing in the $pu.1^{CKO}$ allele. This conclusion was further validated by sequencing analysis of the $pu.1^{CKO}$ transcripts (Fig. 2H and S1D). To confirm that the $pu.1^{CKO}$ allele indeed abolished the function of Pu.1, we outcrossed the $pu.1^{CKO}$ fish with the $pu.1^{\Delta 839}$ mutants, and as anticipated, the development of embryonic microglia was completely blocked in the $pu.1^{cKO/\Delta 839}$ embryos (Fig. 2I and J), a phenotype recapitulating the defect of the $pu.1^{\Delta 839}$

homozygous mutants (Yu et al., 2017). These data demonstrate that the *pu.1*^{KI} allele works very well and serves as a useful tool to explore the role of Pu.1 in adult microglia survival and maintenance.

Conditional inactivation of Pu.1 leads to chronic elimination of microglia in adult zebrafish

To investigate the role of Pu.1 in the survival and maintenance of microglia in adult zebrafish, we crossed the *pu.1*^{KI} fish with the leukocyte-specific *Tg(coro1a:CreER)* line and the *pu.1*$^{\Delta 839}$ mutants to generate *pu.1*$^{KI/+}$*;Tg(coro1a:CreER)* and *pu.1*$^{KI/\Delta 839}$*;Tg(coro1a:CreER)* fish. We then intraperitoneally injected 3 doses of 4-OHT into these adult fish and collected the brain samples at 8 dpi, 1 month post injection (mpi), and 3 mpi for the quantification of microglia number after cryo-section and eGFP/DsRed immuno-staining (Fig. 3A, upper panel). As shown in Fig. S2, at 8 dpi, DsRed^{+} cells were readily detected in the brains of both *pu.1*$^{KI/+}$*;Tg(coro1a:CreER)* and *pu.1*$^{KI/\Delta 839}$*;Tg(coro1a:CreER)* fish, and their number and proportion were comparable between the two genotypes (Fig. 3B and C), suggesting that Pu.1 is not required for the survival of microglia as well as DCs. However, at 1 mpi, the number and proportion of DsRed^{+} cells in the brains of the *pu.1*$^{KI/\Delta 839}$*;Tg(coro1a:CreER)* fish, which represent *pu.1*-null cells, began to decline and were dramatically reduced by 3 mpi (Fig. 3A-C). Likewise, the number and proportion of DsRed^{+} cells in the retina and spinal cord were also significantly reduced in the *pu.1*$^{KI/\Delta 839}$*;Tg(coro1a:CreER)* fish by 3 mpi (Fig. S3). Since microglia are the major population of the *coro1a*$^{+}$ cells in the brain and spinal cord and the exclusive population in the retina (Wu et al., 2020), the reduction of DsRed^{+} cells in the *pu.1*$^{KI/\Delta 839}$*;Tg(coro1a:CreER)* fish at 1 mpi and 3 mpi are mainly attributed to the loss of microglia. Hence, we conclude that that Pu.1 is indispensable for the long-term maintenance of microglia in adult zebrafish.

Surprisingly, when we analyzed the microglia in the brains of adult *pu.1*$^{\Delta 839/\Delta 839}$*;TgBAC(ccl34b.1:eGFP)* null mutants, we found that the number of microglia (ccl34b.1-eGFP^{+}) in the null mutants was comparable to that in the *pu.1*$^{\Delta 839/+}$*;TgBAC(ccl34b.1:eGFP)* siblings (Fig. 3D-E), indicating that *pu.1*-deficient microglia are intrinsically viable and their elimination only occurs in a mosaic condition, in which microglia with a single copy of *pu.1* allele co-exist. We reasoned that intrinsic viability of *pu.1*-deficient microglia in *pu.1*$^{\Delta 839/\Delta 839}$ null mutants is likely attributed to the presence of *spi-b* (also known as *spi1-like* or *spi1a*), which has been shown to play a compensatory role for Pu.1 in microglia early development (Yu et al., 2017). Indeed, conditional inactivation of Pu.1 in the *spi-b*$^{\Delta 232/\Delta 232}$ null mutants led to a rapid depletion of microglia by apoptosis within several days (Fig. S4 and Fig. S5), indicating that Pu.1 and Spi-b indeed act redundantly to regulate the survival of adult microglia. However, as *spi-b* could not fully compensate the function of *pu.1*, *pu.1*-deficient microglia (DsRed^{+}) in mosaic condition are gradually eliminated, due to their less competitiveness compared to those (eGFP^{+}) with a single copy of *pu.1* allele. Based on these

observations, we conclude that the maintenance of microglia in adult zebrafish is regulated by the dosage of Pu.1.

The chronic elimination of *pu.1*-deficient microglia in mosaic condition is Tp53-dependent

To reveal the cellular basis underlying the chronic elimination of *pu.1*-deficient microglia in mosaic condition, we treated the adult *pu.1*$^{KI/\Delta 839}$*;Tg(coro1a:CreER)* fish with 4-OHT to inactivate Pu.1. At 26 dpi, the 4-OHT-treated fish were then injected 5 doses (one dose daily) of BrdU and the brain samples were collected 24 hours later for BrdU and TUNEL staining respectively (Fig. 4A). Quantification results showed that the BrdU incorporation rate of DsRed^{+} cells (*pu.1*-deficient cells) in the brains of the *pu.1*$^{KI/\Delta 839}$*;Tg(coro1a:CreER)* fish was significantly lower than that of eGFP^{+} cells (Fig. 4B). In this assay, the 4-OHT-treated *pu.1*$^{KI/+}$*;Tg(coro1a:CreER)* fish were included as the control, and as expected, the BrdU incorporation rates of the DsRed^{+} and eGFP^{+} microglia in control fish were comparable (Fig. 4B). In parallel, we also found that the percentage of TUNEL^{+}DsRed^{+} microglia in the 4-OHT-treated *pu.1*$^{KI/\Delta 839}$*;Tg(coro1a:CreER)* fish was significantly higher than that of TUNEL^{+}GFP^{+} cells (Fig. 4C), while the percentage of TUNEL^{+}DsRed^{+} cells and TUNEL^{+}GFP^{+} cells in the control *pu.1*$^{KI/+}$*;Tg(coro1a:CreER)* fish was comparable (Fig. 4C). These results indicate that conditional inactivation of Pu.1 in adult zebrafish leads to the impairment of cell proliferation and cell death of *pu.1*-deficient DsRed^{+} microglia in mosaic condition, presumably due to cell competition from eGFP^{+} microglia harboring a single copy of *pu.1*.

To uncover the key downstream targets that mediate the chronic elimination of *pu.1*-deficient DsRed^{+} microglia in mosaic condition, we isolated DsRed^{+} and eGFP^{+} microglia from the 4-OHT-treated *pu.1*$^{KI/\Delta 839}$*;Tg(coro1a:CreER)* fish at 3 mpi and performed transcriptomic analysis (Fig. 4D). Among the differential expressed genes (DEGs), the tumor suppressor gene *tp53* was one of the top targeted genes robustly upregulated in *pu.1*-deficient DsRed^{+} microglia (Fig. 4E-F). Interestingly, recent studies have been revealed that, in addition to regulating cell cycle arrest and apoptosis in DNA damage response (Ou and Schumacher, 2018; Vaddavalli and Schumacher, 2022), Tp53 are also shown to be involved in cell competition regulation in both hematopoietic and non-hemopoietic tissues (Bondar and Medzhitov, 2010; Zhang et al., 2017). Hence, we speculated that the cell competition-mediated chronic elimination of *pu.1*-deficient microglia was likely dependent on Tp53. To support this hypothesis, we conditional inactivated Pu.1 to generate mosaic microglia populations in the *tp53*-deficient mutant background and asked if loss of Tp53 could rescue the microglia phenotype (Fig. 4G, upper panel). Indeed, results showed that the number of *pu.1*-deficient DsRed^{+} microglia in the 4-OHT-treated *pu.1*$^{KI/\Delta 839}$*;tp53*$^{-/-}$*;Tg(coro1a:CreER)* fish was significantly restored compared with *pu.1*$^{KI/\Delta 839}$*;Tg(coro1a:CreER)* control fish (Fig. 4G-I). Collectively, these results demonstrate that the chronic elimination of *pu.1*-deficient microglia in mosaic condition is mediated,

at least in part, by the elevation of Tp53 activity, which leads to the reduced proliferation and excessive death of these microglia.

Dosage-dependent regulation of microglia maintenance by PU.1 is evolutionarily conserved in mice

The above data have demonstrated that the long-term maintenance of microglia in adult zebrafish is regulated by Pu.1 in a dosage-dependent manner. We next wondered whether this mechanism is evolutionarily conserved from teleost to mammals. To address this issue, we first examined the expression of *Pu.1* and *Spi-b* in adult murine microglia. Quantitative RT-PCR revealed that in contrast to the robust expression of *Pu.1*, *Spi-b* was almost undetectable in microglia (Fig. S6A). We therefore focused on *Pu.1* and generated a $Pu.1^{Fl}$ allele, in which the exon 2 of *Pu.1* gene is flanked by loxP (Fig. S6B-C). The $Pu.1^{Fl}$ mice were then crossed with the $Cx3cr1^{CreER\text{-}YFP}$ strain (Yona et al., 2013) to generate $Pu.1^{Fl/+};Cx3cr1^{CreER}$ and $Pu.1^{Fl/Fl};Cx3cr1^{CreER}$ mice for conditional PU.1 inactivation study (Fig. 5A).

To investigate whether microglia maintenance in adult mice requires PU.1, we intraperitoneally injected tamoxifen (TAM) into the $Pu.1^{Fl/+};Cx3cr1^{CreER}$ *and* $Pu.1^{Fl/Fl};Cx3cr1^{CreER}$ mice, and collected the brain samples at 7 dpi for cryo-section and IBA1 staining (Fig. 5A, upper panel). As expected, without TAM, the number of the $IBA1^{+}$ microglia showed no difference in the brain of $Pu.1^{Fl/+};Cx3cr1^{CreER}$ *and* $Pu.1^{Fl/Fl};Cx3cr1^{CreER}$ mice (Fig. S6D-E). However, after TAM injection, the number of the $IBA1^{+}$ microglia in $Pu.1^{Fl/Fl};Cx3cr1^{CreER}$ mice were drastically reduced compared to that in $Pu.1^{Fl/+};Cx3cr1^{CreER}$ mice (Fig. 5A-C), suggesting that PU.1 is indeed required for the survival of adult microglia, which is similar to the double depletion of *pu.1* and *spi-b* in zebrafish (Fig. S4). To further explore whether partial loss of PU.1 activity could reduce the competitiveness of microglia and impairs the long-term maintenance of microglia in mice, we intraperitoneally injected sub-dosage of TAM into adult $Pu.1^{Fl/+};Cx3cr1^{CreER}$ mice to generate mosaic microglia populations for long-term tracing. To quantify the proportion of $Pu.1^{KO/+}$ microglia and $Pu.1^{Fl/+}$ microglia, we sorted YFP^{+} microglia from TAM-injected $Pu.1^{Fl/+};Cx3cr1^{CreER}$ mice at different time windows and amplified $Pu.1^{KO}$ and $Pu.1^{Fl}$ alleles in the gDNA pool by PCR analysis for T-clone quantification (Fig. 5D). As shown in Fig. 5E-F, while the percentage of $Pu.1^{KO/+}$ microglia was comparable to $Pu.1^{Fl/+}$ microglia at 3 dpi, it was dramatically reduced by 3 mpi, suggesting that removal of a single copy of *Pu.1* leads to the chronic elimination of $Pu.1^{KO/+}$ microglia, which appears to occur only in the presence of the WT $Pu.1^{Fl/+}$ microglia, as PU.1 heterozygous mice show no difference in the viability of tissue resident macrophages (Karpurapu et al., 2011). Collectively, these results indicate that the dosage-dependent cell competition-mediated regulation of microglia maintenance by SPI1/PU.1 is evolutionarily conserved from teleost to mammals.

Discussion

In the present study, to explore the role of Pu.1 in microglia survival and maintenance, we established a visible conditional knockout *pu.1*^{KI} allele in zebrafish via the non-homologous end joining (NHEJ)-mediated knock-in method. Actually, conditional inactivation of targeted genes has not been widely applied in zebrafish, possibly due to the difficulty or low efficiency to generate loxP-flanked alleles. Compared to homologous recombination (HR), NHEJ-mediated knock-in of reporter gene has been shown to display 10-fold higher efficiency (Auer et al., 2014; Li et al., 2015). In our case, the germline transmission to F1 generation for *pu.1*^{KI} allele is around 15% (Fig. S1). Meanwhile, in our investigation, we noted that the efficiency of Cre-mediated excision of loxP sites at the *pu.1* locus in zebrafish (Fig. 3) appears much lower than that in mouse (Fig. 5). Although it remains to be further validated whether this observation is a general phenomenon, it does highlight the necessity and significance of chimera study of interested genes. In our *pu.1*^{KI} allele, the expression of DsRed directly indicates Cre-mediated excision and helps us distinguish the mutant cells from their sibling cells, which serves as a good example for chimera study in the future. Moreover, our knock-in allele can also be simply regarded as a loxP-flanked fluorescent reporter line, which not only facilitates the labeling of cells that express gene of interest, but also can be used in combination with the LEGO-IR system (Xu et al., 2015) to trace the fate of these cells. Thus, due to the high integration efficiency of donor DNA fragment and the multifaceted applications of the labeling strategy, we anticipated that our knock-in system would be a powerful tool and broadly be adopted in the fields of genetics, developmental biology and cell biology for the chimeric study of interested genes and fate mapping of interested cells in the future.

Via EdU pulse-chase labelling assay, we found that the daily turnover rate of microglia in adult zebrafish is about 2.5%, much higher than that reported in mice and human (Lopez-Atalaya et al., 2018). These disparities might be explained by several reasons. First, it is well recognized that zebrafish manifest much stronger regeneration capability than mammals. As such, differentiated cells, like cardiomyocytes and hair cells in zebrafish are in general more proliferative than those in mammals (Chen et al., 2019; Marques et al., 2019). In this regard, microglia in zebrafish might be pre-coded both genetically and epigenetically to be more proliferative. Second, microglia turnover could potentially be affected by the distinct efferocytotic burdens via the lysosome pathway, as lysosome has been known to be a convergent point for many biological process, including metabolism, cellular senescence, DNA repair, ER stress and even apoptosis (Franco-Juárez et al., 2022; Perera and Zoncu, 2016). Indeed, efferocytosis of apoptotic cells has previously been shown to elicit NOX2 assembly and promote ROS production (Yvan-Charvet et al., 2010), which in turn triggers cell death via induction of lysosome damage (Patra et al., 2023; Wang et al., 2018). The more

regenerative environment in zebrafish might be accompanied by higher frequency of cell death, which could lead to the increase of efferocytotic burdens of microglia, thereby accelerating the turnover of microglia. Further studies will be required to clarify this issue.

Our results revealed that the survival and maintenance microglia are highly sensitive to the dosage of PU.1/SPI1 in both teleost and mammals. Interestingly, a previous study reported that hetero- or homozygosity of PU/ER(T) allele, in which the estrogen receptor (ER) ligand binding domain-G525R is fused with the full-length PU.1 to block its nucleus translocation, showed no effect on the viability of alveolar macrophages (Karpurapu et al., 2011). This contradictory result might potentially result from the leakiness of ER, which was incapable to fully retain PU.1 in cytoplasm. A recent work found that conditional inactivation of PU.1 by feeding the animals with tamoxifen-containing diet in the Alzheimer's disease model CK-p25 mice led to a 33% reduction in microglia number at their young ages. Although the authors considered prevention of microgliosis as a result of the amelioration of neuroinflammation (Ralvenius et al., 2023), it could also been interpreted by the direct involvement of PU.1 in microglia survival and maintenance, as our data clearly demonstrate that conditional ablation of the PU.1 in mice or Pu.1/Spi-b in zebrafish leads to the rapid depletion of microglia in the brain (Fig. 5; Fig. S4). As PU.1 is a master regulator that controls the expression of series of genes required for macrophage/microglia development (Satoh et al., 2014), rapid death of *Pu.1*-null microglia might probably be caused by the orchestration of multiplex factors, including the downregulation of colony-stimulating factor 1 receptor (*Csf1r*) (the essential regulator controlling the survival and maintenance of microglia in both mice and zebrafish) (Elmore et al., 2014; Yu et al., 2023), the loss of anti-apoptotic genes, such as BCL2A1 (Jenal et al., 2010), and absence of other genes that maintain the integrity of cells. Intriguingly, differing from the rapid death of microglia after complete inactivation of PU.1 or Pu.1/Spi-b, microglia with a partial loss of PU.1 or Pu.1 are chronically eliminated only in the mosaic condition via cell competition, in which the microglia with WT *Pu.1* or a single copy of *pu.1* are present (Fig. 3 and Fig. 5). Moreover, we further showed that the chronic elimination of *pu.1*-dificent microglia in zebrafish is mediated by Tp53-dependent cell competition, which has been shown to depend on the relative level of Tp53 in competing cells (Bondar and Medzhitov, 2010; Zhang et al., 2017). These findings suggest that the dosage of PU.1/Pu.1 may serve as a checkpoint to determine the fitness of microglia. It will be of great interest to explore the upstream events that modulate *PU.1*/*pu.1* expression during microglia turnover.

Materials and Methods

Zebrafish

Zebrafish were maintained according to standard protocol as described previously (Westerfield, 2000). AB wild-type, *pu.1*$^{\Delta 839}$ (Yu et al., 2017), *spi-b*$^{\Delta 232}$ (Yu et al., 2017), *tp53*^{M214K} (Berghmans et

al., 2005), *pu.1*^{KI} (short for *pu.1*^{KI}-GFP), *pu.1*^{CKO} (short for *pu.1*^{KI}-DsRed), *TgBAC(ccl34b.1:eGFP)* (Wu et al., 2020), *Tg(coro1a:CreER*^{T2}*)*^{sz101tg}, *Tg(mpeg1:loxP-DsRedx-loxP-eGFP, shorted as LRLG)*^{hkz015t} (Xu et al., 2016) were used in this study.

Mouse strains

Pu.1^{Fl} (No.T010980, purchased from GemPharmatech Co.,Ltd) and *Cx3cr1*$^{CreER\text{-}EYFP}$ (Stock No. 021160) (Yona et al., 2013) were used in this study. All animal experiments and procedures were proved by Ethics Committee for the Welfare of Laboratory Animals in Shenzhen PKU-HKUST Medical Center.

Generation of *pu.1*^{KI} allele

Donor plasmid was modified based on the reported Th-KI plasmid (Li et al., 2015). In brief, DNA fragments containing *pu.1* exon 4 to exon 6 and the 3' downstream fragment were cloned from cDNA and genomic DNA libraries respectively and inserted into the plasmid containing P2A-GFP, P2A-Dsred and loxP elements. sgRNA was designed in the intron 3~4 of *pu.1* with the online website Crisprscan (https://www.crisprscan.org/). It was transcribed by MEGAshortscript Kit (AM1354, Invitrogen) from PCR product which was amplified following reported protocol (Vejnar et al., 2016). Then Cas9 mRNA (700 ng/ul), sgRNA (70 ng/ul) and donor plasmid (15 ng/ul) were mixed and injected into zebrafish embryos at one-cell stage. Embryos with GFP signal were selected at 3 dpf and raised to adulthood for germline transmission.

Cryo-section

Adult fish were anesthetized on ice. The tissue was dissected and fixed in 4% PFA at 4℃ overnight. After being washed with phosphate-buffered saline (PBS) at room temperature for 1 day, the tissues were dehydrated with 30% sucrose at 4℃ overnight, then soaked in coagulating solution (optimal cutting temperature compound, OCT) and subjected to cryosection with 30-μm thickness.

EdU and BrdU incorporation assays, TUNEL staining, and immunostaining

EdU and BrdU incorporation assays were conducted as previously reported (Yu et al., 2023). In brief, EdU (A10044, Invitrogen) or BrdU (B5002, Sigma-Aldrich) was dissolved in PBS to the final concentration of 10 mg/ml. 5 ul EdU or BrdU was intraperitoneally (i.p.) injected into adult zebrafish each time. Brain samples were dissected at 1 day post injection and fixed in 4% PFA for cryosection.

EdU detection was conducted with (Click-iT™ EdU Cell Proliferation Kit for Imaging, Alexa Fluor™ 647 dye, Invitrogen, C10340) according to the manufacturer's instructions. For BrdU detection, samples were treated with 2M HCl for half an hour and then stained with the BrdU antibody. TUNEL staining was performed with TUNEL BrightGreen Apoptosis Detection Kit (A112, Vazyme) according to the manufacturer's instructions. Antibody staining was performed after EdU/BrdU and TUNEL detection. Primary antibodies used in this study were mouse anti-BrdU antibody (11170376001, Roche), goat anti-GFP (ab6658, Abcam), rabbit anti-DsRed (632496, Clontech), rabbit anti-Lcp1 (Jin et al., 2009), rabbit anti-Pu.1 (Jin et al., 2012) and rabbit anti-IBA1 (019-19741, FUJIFILM Wako) antibodies.

Tamoxifen injection

4-Hydroxytamoxifen (4-OHT, H7904, Sigma) was dissolved in ethanol to final concentration of 10 mM. For adult fish, 1 ul 4-OHT was i.p. injected into each fish for 3 times. For adult mice, tamoxifen (T5648, Sigma) was dissolved in corn oil to final concentration of 20 mg/ml and i.p. injected into the mice with 35 mg/kg (sub-dosage) or 150 mg/kg (over-dosage).

Neutral red staining

Neutral red staining was performed as previously described (Herbomel et al., 2001).

Cy5-Annexin V treatment

Annexin V-Cy5 Reagent (1013, Biovision) solution was directly injected into brain ventricle of 3 dpf larva and immediately imaged by confocal microscope.

Imaging

Fluorescent signals from live reporter lines or immunostaining were imaged under a Leica SP8 confocal microscope or a Zeiss LSM980 confocal microscope. The objectives HC PL APO 203/0.70 DRY (Leica) and Plan-Apochromat 20×/0.8 M27 (Zeiss) were used in this study.

cDNA preparation and RNA-seq

Cell suspensions were prepared as previously described (Yu et al., 2017). Cells of interest were manually picked under the fluorescent microscope (Nikon Ti-S) equipped with the micro-manipulator

(NT-88-V3, Nikon). Subsequently, picked cells were transferred by the glass needle to lysis buffer (mainly including Triton X-100 and RNase inhibitor) for thorough vertex. Then the cell lysate was used for reverse-transcription and amplification with the Smart-Seq2 method (Picelli et al., 2014) to generate the cDNA library. cDNA was sent to Novogene Company for Illumina sequencing with an average depth of 6×10^6 raw reads per sample.

Mice microglia isolation

Adult mice brain was dissected and cut into small pieces. They were dissociated into single-cell suspensions with Adult Brain Dissociation Kit (130-107-677, Miltenyi Biotec) according to the manufacturer's instructions. Then Myelin Removal Beads II (130-96-733, Miltenyi Biotec) were used to remove myelin debris from single-cell suspensions. YFP^+ Microglia were sorted from suspensions by FACS Aria IIIu. The sorted microglia were lysed by proteinase K to extract DNA or TRIzol to extract RNA.

TA clone assay

Pu.1^{Fl} and *Pu.1*^{KO} alleles were amplified by PCR from the genomic DNA. The common forward primer was 5'-GCATCGCATTGTCTGAGTAGGT-3. The reverse primers were 5'-AAATCTGCCTGGGTGACCTTC-3' for *Pu.1*^{Fl} and 5'-ACACAACGGGTTCTTCTGTTAG-3' for *Pu.1*^{KO}. The PCR products for *Pu.1* ^{Fl} and *Pu.1* ^{KO} alleles were 248 bp and 129 bp respectively. PCR products were ligated to pUCm-T vector (B522211, Sangon) with Blunt/TA Ligase Master Mix (M0367S, NEB) according to the manufacturer's instructions. The clones containing ligated plasmids were amplified with M13F (5'-GTTGTAAAACGACGGCCAG-3') and M13R (5'-CAGGAAACAGCTATGAC-3'). The PCR products for *Pu.1* ^{Fl} and *Pu.1* ^{KO} alleles were 437 bp and 315 bp respectively. Clones of *Pu.1*^{Fl} and *Pu.1*^{KO} alleles were distinguished by the size of PCR products.

Quantitative PCR

cDNA was synthesized from extracted RNA with SuperScript™ III Reverse Transcriptase kit (18080093, Invitrogen). Quantitative PCR was performed with iTaq™ Universal SYBR® Green Supermix (1725121, Bio-rad) on a CFX96 Dx Instrument (Bio-rad) and analyzed using the ΔΔCt method. The following primers were used to determine the expression of *DsRed* and *pu.1* from *pu.1*^{CKO} allele: *DsRed*, 5'-GATCTATCGACCACCAATGGAG-3' (*pu.1*-161FP)/ 5'-GCCGTTCACGGAGCCCTCCAT-3' (DsRed-72RP); *pu.1*, 5'-GATCTATCGACCACCAATGGAG-3' (*pu.1*-161FP)/ 5'-CGCATGTAGTGACTGCACGC-3' (*pu.1*-357RP). The following primers were used to determine the expression of *Pu.1* and *Spi-b* in mouse microglia: *Gapdh*, 5'-

TGTGTCCGTCGTGGATCTGA-3'/5'-TTGCTGTTGAAGTCGCAGGAG-3'; *Pu.1*, 5'-GAGGTGTCTGATGGAGAAGCTG-3'/5'-ACCCACCAGATGCTGTCCTTCA-3'; *Spi-b*, 5'-AGGAGTCTTCTACGACCTGGAC-3'/5'-GGAGTGGCTAAAGGCAGCAGTA-3'.

Statistics

Statistics were analyzed using the 2-tailed Student t test. A result was considered significant if P <.05. Values represent mean ± standard error of the mean.

Acknowledgements: We thank Dr. Keng Chen and Dr. Keyu Chen in Shenzhen Bay Laboratory for their assistance in the Fluorescent-activated cell sorting (FACS) of mouse microglia, and thank Prof. Zilong Wen in South University of Science and Technology of China and Prof. Jin Xu in South China University of Technology for their kind suggestions and revises for this manuscript.

Fundings: This work is supported by the Major Program of Shenzhen Bay Laboratory (S201101002) and Shenzhen Medical Academy of Research and Translation (SMART) 2023 Shenzhen Medical Research Funding (B2302034).

References

Ajami, B., Bennett, J.L., Krieger, C., Tetzlaff, W., and Rossi, F.M.V. (2007). Local self-renewal can sustain CNS microglia maintenance and function throughout adult life. Nature neuroscience *10*, 1538-1543.

Askew, K., Li, K., Olmos-Alonso, A., Garcia-Moreno, F., Liang, Y., Richardson, P., Tipton, T., Chapman, M.A., Riecken, K., Beccari, S., *et al.* (2017). Coupled Proliferation and Apoptosis Maintain the Rapid Turnover of Microglia in the Adult Brain. Cell reports *18*, 391-405.

Auer, T.O., Duroure, K., De Cian, A., Concordet, J.P., and Del Bene, F. (2014). Highly efficient CRISPR/Cas9-mediated knock-in in zebrafish by homology-independent DNA repair. Genome research *24*, 142-153.

Berghmans, S., Murphey, R.D., Wienholds, E., Neuberg, D., Kutok, J.L., Fletcher, C.D.M., Morris, J.P., Liu, T.X., Schulte-Merker, S., Kanki, J.P., *et al.* (2005). *tp53* mutant zebrafish develop malignant peripheral nerve sheath tumors. Proceedings of the National Academy of Sciences *102*, 407-412.

Bondar, T., and Medzhitov, R. (2010). p53-Mediated Hematopoietic Stem and Progenitor Cell Competition. Cell stem cell *6*, 309-322.

Bruttger, J., Karram, K., Wörtge, S., Regen, T., Marini, F., Hoppmann, N., Klein, M., Blank, T., Yona, S., Wolf, Y., *et al.* (2015). Genetic Cell Ablation Reveals Clusters of Local Self-Renewing Microglia in the Mammalian Central Nervous System. Immunity *43*, 92-106.

Cao, H., Zhou, X., Chen, Y., Ip, F.C.F., Chen, Y., Lai, N.C.H., Lo, R.M.N., Tong, E.P.S., Mok, V.C.T., Kwok, T.C.Y., *et al.* (2022). Association of SPI1 Haplotypes with Altered SPI1 Gene Expression and Alzheimer's Disease Risk. J Alzheimers Dis *86*, 1861-1873.

Chen, Y., Zhang, S., Chai, R., and Li, H. (2019). Hair Cell Regeneration. In Hearing Loss: Mechanisms, Prevention and Cure, H. Li, and R. Chai, eds. (Singapore: Springer Singapore), pp. 1-16.

Colonna, M., and Butovsky, O. (2017). Microglia Function in the Central Nervous System During Health and Neurodegeneration. Annual review of immunology *35*, 441-468.

Elmore, Monica R.P., Najafi, Allison R., Koike, Maya A., Dagher, Nabil N., Spangenberg, Elizabeth E., Rice, Rachel A., Kitazawa, M., Matusow, B., Nguyen, H., West, Brian L., *et al.* (2014).

Colony-Stimulating Factor 1 Receptor Signaling Is Necessary for Microglia Viability, Unmasking a Microglia Progenitor Cell in the Adult Brain. Neuron *82*, 380-397.
Franco-Juárez, B., Coronel-Cruz, C., Hernández-Ochoa, B., Gómez-Manzo, S., Cárdenas-Rodríguez, N., Arreguin-Espinosa, R., Bandala, C., Canseco-Ávila, L.M., and Ortega-Cuellar, D. (2022). TFEB; Beyond Its Role as an Autophagy and Lysosomes Regulator. Cells *11*, 3153.
Füger, P., Hefendehl, J.K., Veeraraghavalu, K., Wendeln, A.C., Schlosser, C., Obermüller, U., Wegenast-Braun, B.M., Neher, J.J., Martus, P., Kohsaka, S., *et al.* (2017). Microglia turnover with aging and in an Alzheimer's model via long-term in vivo single-cell imaging. Nature neuroscience *20*, 1371-1376.
Ginhoux, F., Greter, M., Leboeuf, M., Nandi, S., See, P., Gokhan, S., Mehler, M.F., Conway, S.J., Ng, L.G., Stanley, E.R., *et al.* (2010). Fate mapping analysis reveals that adult microglia derive from primitive macrophages. Science *330*, 841-845.
Glass, C.K., Saijo, K., Winner, B., Marchetto, M.C., and Gage, F.H. (2010). Mechanisms underlying inflammation in neurodegeneration. Cell *140*, 918-934.
Gomez-Nicola, D., and Perry, V.H. (2015). Microglial Dynamics and Role in the Healthy and Diseased Brain: A Paradigm of Functional Plasticity. The Neuroscientist *21*, 169-184.
Herbomel, P., Thisse, B., and Thisse, C. (2001). Zebrafish early macrophages colonize cephalic mesenchyme and developing brain, retina, and epidermis through a M-CSF receptor-dependent invasive process. Developmental biology *238*, 274-288.
Hoshijima, K., Jurynec, Michael J., and Grunwald, David J. (2016). Precise Editing of the Zebrafish Genome Made Simple and Efficient. Developmental cell *36*, 654-667.
Huang, K.L., Marcora, E., Pimenova, A.A., Di Narzo, A.F., Kapoor, M., Jin, S.C., Harari, O., Bertelsen, S., Fairfax, B.P., Czajkowski, J., *et al.* (2017). A common haplotype lowers PU.1 expression in myeloid cells and delays onset of Alzheimer's disease. Nature neuroscience *20*, 1052-1061.
Jenal, M., Batliner, J., Reddy, V.A., Haferlach, T., Tobler, A., Fey, M.F., Torbett, B.E., and Tschan, M.P. (2010). The anti-apoptotic gene BCL2A1 is a novel transcriptional target of PU.1. Leukemia *24*, 1073-1076.
Jin, H., Li, L., Xu, J., Zhen, F., Zhu, L., Liu, P.P., Zhang, M., Zhang, W., and Wen, Z. (2012). Runx1 regulates embryonic myeloid fate choice in zebrafish through a negative feedback loop inhibiting Pu.1 expression. Blood *119*, 5239-5249.
Jin, H., Sood, R., Xu, J., Zhen, F., English, M.A., Liu, P.P., and Wen, Z. (2009). Definitive hematopoietic stem/progenitor cells manifest distinct differentiation output in the zebrafish VDA and PBI. Development *136*, 647-654.
Karpurapu, M., Wang, X., Deng, J., Park, H., Xiao, L., Sadikot, R.T., Frey, R.S., Maus, U.A., Park, G.Y., Scott, E.W., *et al.* (2011). Functional PU.1 in macrophages has a pivotal role in NF-κB activation and neutrophilic lung inflammation during endotoxemia. Blood *118*, 5255-5266.
Kierdorf, K., Erny, D., Goldmann, T., Sander, V., Schulz, C., Perdiguero, E.G., Wieghofer, P., Heinrich, A., Riemke, P., Holscher, C., *et al.* (2013). Microglia emerge from erythromyeloid precursors via Pu.1- and Irf8-dependent pathways. Nature neuroscience *16*, 273-280.
Lawson, L.J., Perry, V.H., and Gordon, S. (1992). Turnover of resident microglia in the normal adult mouse brain. Neuroscience *48*, 405-415.
Li, J., Zhang, B.B., Ren, Y.G., Gu, S.Y., Xiang, Y.H., and Du, J.L. (2015). Intron targeting-mediated and endogenous gene integrity-maintaining knockin in zebrafish using the CRISPR/Cas9 system. Cell research *25*, 634-637.
Li, Y., Du, X.-f., Liu, C.-s., Wen, Z.-l., and Du, J.-l. (2012). Reciprocal Regulation between Resting Microglial Dynamics and Neuronal Activity In Vivo. Developmental cell *23*, 1189-1202.
Lopez-Atalaya, J.P., Askew, K.E., Sierra, A., and Gomez-Nicola, D. (2018). Development and maintenance of the brain's immune toolkit: Microglia and non-parenchymal brain macrophages. Dev Neurobiol *78*, 561-579.
Marques, I.J., Lupi, E., and Mercader, N. (2019). Model systems for regeneration: zebrafish. Development *146*.

McKercher, S.R., Torbett, B.E., Anderson, K.L., Henkel, G.W., Vestal, D.J., Baribault, H., Klemsz, M., Feeney, A.J., Wu, G.E., Paige, C.J., *et al.* (1996). Targeted disruption of the PU.1 gene results in multiple hematopoietic abnormalities. The EMBO journal *15*, 5647-5658.
Ou, H.-L., and Schumacher, B. (2018). DNA damage responses and p53 in the aging process. Blood *131*, 488-495.
Patra, S., Patil, S., Klionsky, D.J., and Bhutia, S.K. (2023). Lysosome signaling in cell survival and programmed cell death for cellular homeostasis. Journal of cellular physiology *238*, 287-305.
Perera, R.M., and Zoncu, R. (2016). The Lysosome as a Regulatory Hub. Annual Review of Cell and Developmental Biology *32*, 223-253.
Peri, F., and Nüsslein-Volhard, C. (2008). Live Imaging of Neuronal Degradation by Microglia Reveals a Role for v0-ATPase a1 in Phagosomal Fusion In Vivo. Cell *133*, 916-927.
Picelli, S., Faridani, O.R., Björklund, Å.K., Winberg, G., Sagasser, S., and Sandberg, R. (2014). Full-length RNA-seq from single cells using Smart-seq2. Nature protocols *9*, 171.
Prinz, M., Priller, J., Sisodia, S.S., and Ransohoff, R.M. (2011). Heterogeneity of CNS myeloid cells and their roles in neurodegeneration. Nature neuroscience *14*, 1227-1235.
Ralvenius, W.T., Mungenast, A.E., Woolf, H., Huston, M.M., Gillingham, T.Z., Godin, S.K., Penney, J., Cam, H.P., Gao, F., Fernandez, C.G., *et al.* (2023). A novel molecular class that recruits HDAC/MECP2 complexes to PU.1 motifs reduces neuroinflammation. J Exp Med *220*.
Satoh, J., Asahina, N., Kitano, S., and Kino, Y. (2014). A Comprehensive Profile of ChIP-Seq-Based PU.1/Spi1 Target Genes in Microglia. Gene Regul Syst Bio *8*, 127-139.
Schulz, C., Gomez Perdiguero, E., Chorro, L., Szabo-Rogers, H., Cagnard, N., Kierdorf, K., Prinz, M., Wu, B., Jacobsen, S.E., Pollard, J.W., *et al.* (2012). A lineage of myeloid cells independent of Myb and hematopoietic stem cells. Science *336*, 86-90.
Scott, E.W., Simon, M.C., Anastasi, J., and Singh, H. (1994). Requirement of transcription factor PU.1 in the development of multiple hematopoietic lineages. Science *265*, 1573-1577.
Smith, A.M., Gibbons, H.M., Oldfield, R.L., Bergin, P.M., Mee, E.W., Faull, R.L., and Dragunow, M. (2013). The transcription factor PU.1 is critical for viability and function of human brain microglia. Glia *61*, 929-942.
Sugimoto, K., Hui, S.P., Sheng, D.Z., and Kikuchi, K. (2017). Dissection of zebrafish shha function using site-specific targeting with a Cre-dependent genetic switch. eLife *6*, e24635.
Tay, T.L., Mai, D., Dautzenberg, J., Fernández-Klett, F., Lin, G., Sagar, Datta, M., Drougard, A., Stempfl, T., Ardura-Fabregat, A., *et al.* (2017). A new fate mapping system reveals context-dependent random or clonal expansion of microglia. Nature neuroscience *20*, 793-803.
Vaddavalli, P.L., and Schumacher, B. (2022). The p53 network: cellular and systemic DNA damage responses in cancer and aging. Trends in Genetics *38*, 598-612.
Vejnar, C.E., Moreno-Mateos, M.A., Cifuentes, D., Bazzini, A.A., and Giraldez, A.J. (2016). Optimized CRISPR-Cas9 System for Genome Editing in Zebrafish. Cold Spring Harb Protoc *2016*.
Walton, M.R., Gibbons, H., MacGibbon, G.A., Sirimanne, E., Saura, J., Gluckman, P.D., and Dragunow, M. (2000). PU.1 expression in microglia. J Neuroimmunol *104*, 109-115.
Wang, F., Gómez-Sintes, R., and Boya, P. (2018). Lysosomal membrane permeabilization and cell death. Traffic *19*, 918-931.
Westerfield, M. (2000). The Zebrafish Book: A Guide for the Laboratory Use of Zebrafish (Danio rerio), 4th Edition. University of Oregon Press, Eugene.
Wu, S., Nguyen, L.T.M., Pan, H., Hassan, S., Dai, Y., Xu, J., and Wen, Z. (2020). Two phenotypically and functionally distinct microglial populations in adult zebrafish. Sci Adv *6*.
Xu, J., Wang, T., Wu, Y., Jin, W., and Wen, Z. (2016). Microglia Colonization of Developing Zebrafish Midbrain Is Promoted by Apoptotic Neuron and Lysophosphatidylcholine. Developmental cell *38*, 214-222.
Xu, J., Zhu, L., He, S., Wu, Y., Jin, W., Yu, T., Qu, J.Y., and Wen, Z. (2015). Temporal-Spatial Resolution Fate Mapping Reveals Distinct Origins for Embryonic and Adult Microglia in Zebrafish. Developmental cell *34*, 632-641.

Yona, S., Kim, K.-W., Wolf, Y., Mildner, A., Varol, D., Breker, M., Strauss-Ayali, D., Viukov, S., Guilliams, M., Misharin, A., *et al.* (2013). Fate Mapping Reveals Origins and Dynamics of Monocytes and Tissue Macrophages under Homeostasis. Immunity *38*, 79-91.
Yu, T., Guo, W., Tian, Y., Xu, J., Chen, J., Li, L., and Wen, Z. (2017). Distinct regulatory networks control the development of macrophages of different origins in zebrafish. Blood *129*, 509-519.
Yu, T., Kuang, H., Wu, X., Huang, Y., Wang, J., and Wen, Z. (2023). Cell competition for neuron-derived trophic factor controls the turnover and lifespan of microglia. Science Advances *9*, eadf9790.
Yvan-Charvet, L., Pagler, T.A., Seimon, T.A., Thorp, E., Welch, C.L., Witztum, J.L., Tabas, I., and Tall, A.R. (2010). ABCA1 and ABCG1 Protect Against Oxidative Stress–Induced Macrophage Apoptosis During Efferocytosis. Circulation research *106*, 1861-1869.
Zhang, D.E., Hetherington, C.J., Chen, H.M., and Tenen, D.G. (1994). The macrophage transcription factor PU.1 directs tissue-specific expression of the macrophage colony-stimulating factor receptor. Molecular and cellular biology *14*, 373-381.
Zhang, G., Xie, Y., Zhou, Y., Xiang, C., Chen, L., Zhang, C., Hou, X., Chen, J., Zong, H., and Liu, G. (2017). p53 pathway is involved in cell competition during mouse embryogenesis. Proceedings of the National Academy of Sciences *114*, 498-503.
Zhou, Q., Zhao, C., Yang, Z., Qu, R., Li, Y., Fan, Y., Tang, J., Xie, T., and Wen, Z. (2023). Cross-organ single-cell transcriptome profiling reveals macrophage and dendritic cell heterogeneity in zebrafish. Cell reports *42*.

Figure legends

Figure 1. Characterization of microglia turnover in adult zebrafish. (A) Schematic diagram shows the workflow of EdU pulse experiment in adult *TgBAC(ccl34b.1:eGFP)* zebrafish and the representative images of proliferating microglia (ccl34b.1-eGFP$^+$EdU$^+$) and dendritic cells (DCs) (ccl34b.1-eGFP$^-$Lcp1$^+$EdU$^+$) in the midbrain. **(B)** Quantification of the EdU incorporation proportions in microglia and DCs with different dosages of EdU pulse. **(C)** The daily turnover rate of microglia and DCs calculated by dividing the EdU incorporation rate with EdU pulses. **(D)** Schematic diagram shows the experimental setup for EdU-BrdU double-pulse in adult wild-type fish and the representative images shows two BrdU$^+$ microglia with or without EdU incorporation. **(E)** Comparison of BrdU incorporation proportions in EdU$^+$GFP$^+$ and EdU$^-$GFP$^+$ microglia. n.s., $P > 0.05$ (Student's *t* test).

Figure 2. Generation and characterization of *pu.1^{KI}* allele for visible conditional knockout of *pu.1* gene in zebrafish. (A) Schematic diagrams show the generation of *pu.1^{KI}* allele and the principle for *pu.1* visible conditional knockout. Briefly, the donor plasmid, which contains: (1) the sgRNA target sequence in *pu.1* intron 3~4; (2) the loxP-flanked *pu.1* coding sequence (exon4-6) followed by P2A-eGFP; (3) the splicing acceptor site followed by P2A-DsRed sequence was knocked into the endogenous *pu.1* locus via non-homologous end joining (NHEJ) to generate *pu.1^{KI}*. In principle, the splicing event occurring between E3 and E4 In *pu.1^{KI}* would produce intact Pu.1 and GFP concurrently. After Cre-mediated recombination, removal of *pu.1* E4-6 and splicing of P2A-DsRed sequence in *pu.1^{CKO}* allele leads to the disruption of Pu.1 and fluorescent color change. **(B)** Co-staining of anti-GFP and anti-Pu.1 antibodies on the yolk sac (YS) of 21-hpf *pu.1^{KI}* embryos. **(C)**

Fluorescent imaging of the optic tectum (OT) region of 3-dpf *pu.1*^{KI}*;Tg(mpeg1:LRLG)* embryos. **(D)** Co-staining of anti-GFP and anti-Lcp1 antibodies on the midbrain cross section of adult *pu.1*^{KI} fish. **(E)** Neutral red staining of *pu.1*$^{KI/+}$ and *pu.1*$^{KI/\Delta 839}$ embryos at 3 dpf. **(F)** Quantification of NR^{+} microglia in *pu.1*$^{KI/+}$ and *pu.1* $^{KI/\Delta 839}$ embryos at 3 dpf. **(G)** Fluorescent imaging of the YS region of 30-hpf *pu.1*$^{KI/CKO}$ embryos. **(H)** Chromogram of cDNA sequence from *pu.1*^{CKO} embryos shows the precise splicing of *P2A-DsRed* cassette to *pu.1* E3. **(I)** Neutral red staining of *pu.1*$^{CKO/+}$ and *pu.1*$^{CKO/\Delta 839}$ embryos at 3 dpf. **(J)** Quantification of NR^{+} microglia in *pu.1*$^{CKO/+}$ and *pu.1*$^{CKO/\Delta 839}$ embryos at 3 dpf. Student t test. n.s. = not significant, p>0.05;****P<0.0001.

Figure 3. Conditional knockout of *pu.1* leads to chronic elimination of microglia in adult zebrafish by cell competition. (A) The experimental setup for *pu.1* conditional knockout in adult zebrafish and the representative images of midbrain cross section of *pu.1*$^{KI/+}$*;Tg(coro1a:CreER)* and *pu.1*$^{KI/\Delta 839}$*;Tg(coro1a:CreER)* fish at 3-months post 4-OHT injection (mpi). **(B)** Quantification of the number of DsRed^{+} microglia on the midbrain cross section of *pu.1*$^{KI/+}$*;Tg(coro1a:CreER)* and *pu.1*$^{KI/\Delta 839}$*;Tg(coro1a:CreER)* fish at 8-days post 4-OHT injection (dpi), 1 mpi and 3 mpi. **(C)** Quantification of the proportion of DsRed^{+} microglia on the midbrain cross section of *pu.1*$^{KI/+}$*;Tg(coro1a:CreER)* and *pu.1*$^{KI/\Delta 839}$*;Tg(coro1a:CreER)* fish at 8 dpi, 1 mpi and 3 mpi. **(D)** Representative images show the co-staining of GFP and Lcp1 antibodies on the midbrain cross section of adult *pu.1*$^{\Delta 839/+}$*;TgBAC(ccl34b.1:eGFP)* and *pu.1*$^{\Delta 839/\Delta 839}$*;TgBAC(ccl34b.1:eGFP)* fish. GFP^{+} cells represent microglia, whereas GFP^{-}Lcp1^{+} cells are DCs. **(E)** Quantification of the number of GFP^{+} microglia and GFP^{-}Lcp1^{+} DCs on the midbrain cross section of adult *pu.1*$^{\Delta 839/+}$*;TgBAC(ccl34b.1:eGFP)* and *pu.1*$^{\Delta 839/\Delta 839}$*;TgBAC(ccl34b.1:eGFP)* fish. Student t test. n.s. = not significant, p>0.05;***p<0.001.

Figure 4. Inactivation of Tp53 prevents the elimination of *pu.1*-deficient microglia. (A) The experimental setup for BrdU incorporation and TUNEL assays in *pu.1*$^{KI/+}$*;Tg(coro1a:CreER)* and *pu.1*$^{KI/\Delta 839}$*;Tg(coro1a:CreER)* fish at 1 mpi. **(B)** Quantification of the percentage of BrdU^{+} cells in GFP^{+} and DsRed^{+} microglia in *pu.1*$^{KI/+}$*;Tg(coro1a:CreER)* and *pu.1*$^{KI/\Delta 839}$*;Tg(coro1a:CreER)* fish at 1 mpi. **(C)** Quantification of the percentage of TUNEL^{+} cells in GFP^{+} and DsRed^{+} microglia in *pu.1*$^{KI/+}$*;Tg(coro1a:CreER)* and *pu.1*$^{KI/\Delta 839}$*;Tg(coro1a:CreER)* fish at 1 mpi. **(D)** The experimental setup for the isolation of GFP^{+} and DsRed^{+} microglia from *pu.1*$^{KI/\Delta 839}$*;Tg(coro1a:CreER)* adult brain at 3 mpi for transcriptomic analysis. **(E)** The volcano plot of differential expressed genes (DEG) between GFP^{+} and DsRed^{+} microglia at 3 mpi. **(F)** Relative expression (tpm) of *tp53* in GFP^{+} and DsRed^{+} microglia at 3 mpi. **(G)** The experimental setup for *pu.1* conditional knockout in wild-type and *tp53*$^{-/-}$ adult zebrafish, and the representative images of midbrain cross section of

pu.1$^{KI/\Delta 839}$*;Tg(coro1a:CreER)* and *pu.1*$^{KI/\Delta 839}$*;tp53*$^{-/-}$*;Tg(coro1a:CreER)* fish at 3 mpi. **(H)** Quantification of the number of DsRed^{+}, GFP^{+} and total (DsRed + GFP) microglia in *pu.1*$^{KI/\Delta 839}$*;Tg(coro1a:CreER)* and *pu.1*$^{KI/\Delta 839}$*;tp53*$^{-/-}$*;Tg(coro1a:CreER)* fish at 3 mpi. **(I)** Quantification of the proportion of DsRed^{+} microglia in *pu.1*$^{KI/\Delta 839}$*;Tg(coro1a:CreER) and pu.1*$^{KI/\Delta 839}$*;tp53*$^{-/-}$*;Tg(coro1a:CreER)* fish at 90 dpi.

Figure 5. Dosage-dependent regulation of microglia maintenance by Pu.1/Spi1 is evolutionary conserved in mice. (A) The experimental setup for *Pu.1* conditional knockout in adult mice. **(B)** Representative images of IBA1 and DAPI co-staining in the cortex, hippocampus and thalamus of *Pu.1*$^{Fl/+}$*;Cx3cr1*^{CreER} and *Pu.1*$^{Fl/Fl}$*;Cx3cr1*^{CreER} mice at 7 dpi. **(C)** Quantification of the density of IBA1^{+} microglia in the cortex, hippocampus and thalamus of *Pu.1*$^{Fl/+}$*;Cx3cr1*^{CreER} and *Pu.1*$^{Fl/Fl}$*;Cx3cr1*^{CreER} mice at 7 dpi. **(D)** The experimental setup for conditional knockout of *Pu.1* in *Pu.1*$^{Fl/+}$*;Cx3cr1*^{CreER} mice, and the subsequent PCR detection and T-clone quantification of *Pu.1*^{Fl} and *Pu.1*^{KO} alleles in sorted YFP^{+} microglia. **(E)** Gel image shows the relative intensity of amplified DNA bands of *Pu.1*^{Fl} and *Pu.1*^{KO} alleles in microglia sorted from *Pu.1*$^{Fl/+}$*;Cx3cr1*^{CreER} mice at different stages post TAM injection. (**F**) Quantification of the percentage of *Pu.1*^{KO} allele by T-clone assay. Student t test. *p<0.05, ***p<0.001;****p<0.0001.

Figure 1

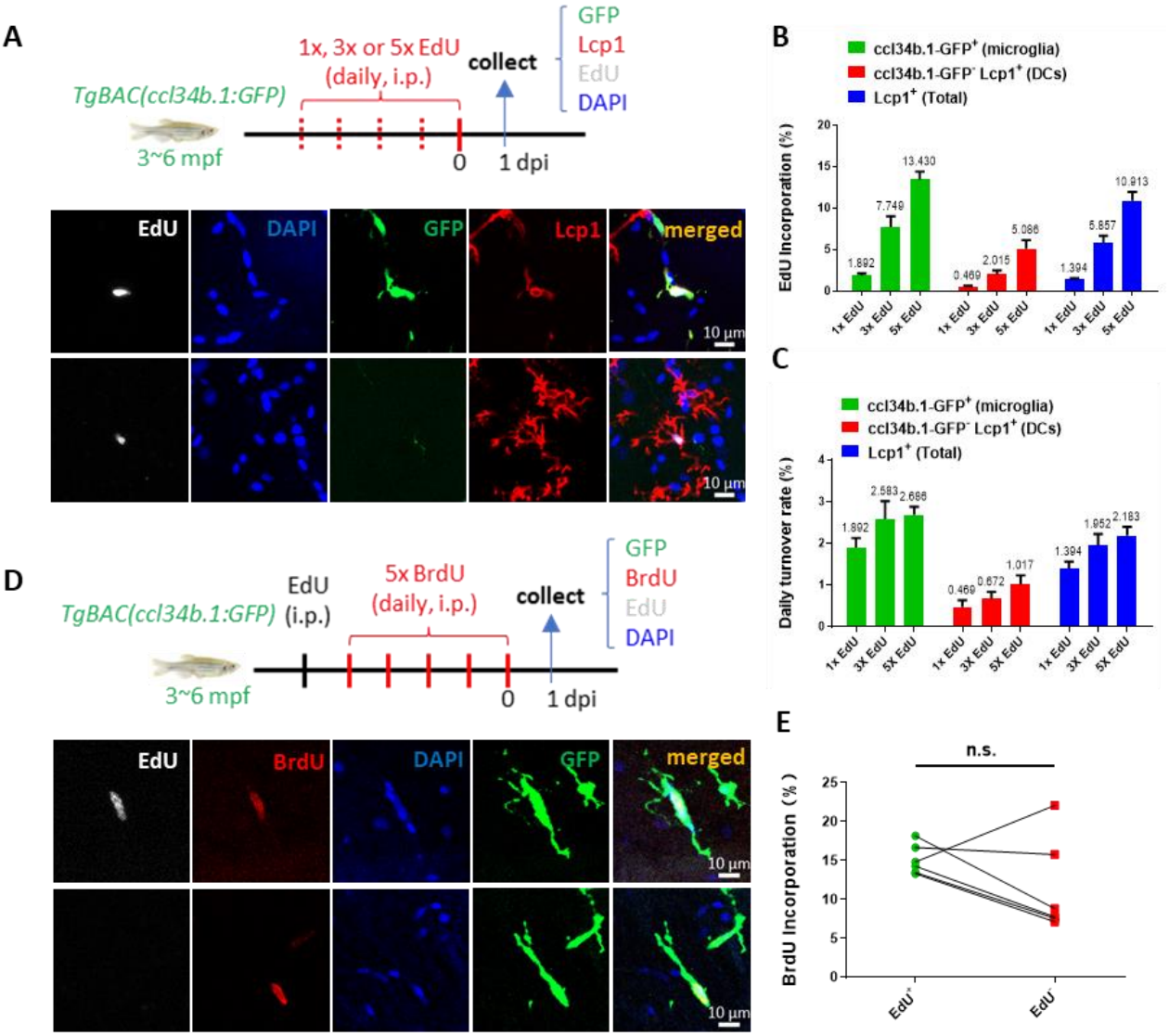
A
1x, 3x or 5x EdU
(daily, i.p.)
collect
GFP
Lcp1
EdU
DAPI
TgBAC(ccl34b.1:GFP)
3~6 mpf
0
1 dpi
EdU
DAPI
GFP
Lcp1
merged
10 μm
B
ccl34b.1-GFP+ (microglia)
ccl34b.1-GFP- Lcp1+ (DCs)
Lcp1+ (Total)
EdU Incorporation (%)
1.892
7.749
13.430
0.469
2.015
5.086
1.394
5.857
10.913
1x EdU
3x EdU
5x EdU
C
Daily turnover rate (%)
1.892
2.593
2.686
0.469
0.672
1.017
1.394
1.952
2.183
D
EdU
(i.p.)
5x BrdU
(daily, i.p.)
collect
GFP
BrdU
EdU
DAPI
TgBAC(ccl34b.1:GFP)
3~6 mpf
0
1 dpi
EdU
BrdU
DAPI
GFP
merged
10 μm
E
n.s.
BrdU Incorporation (%)
EdU-
EdU+

Figure 2

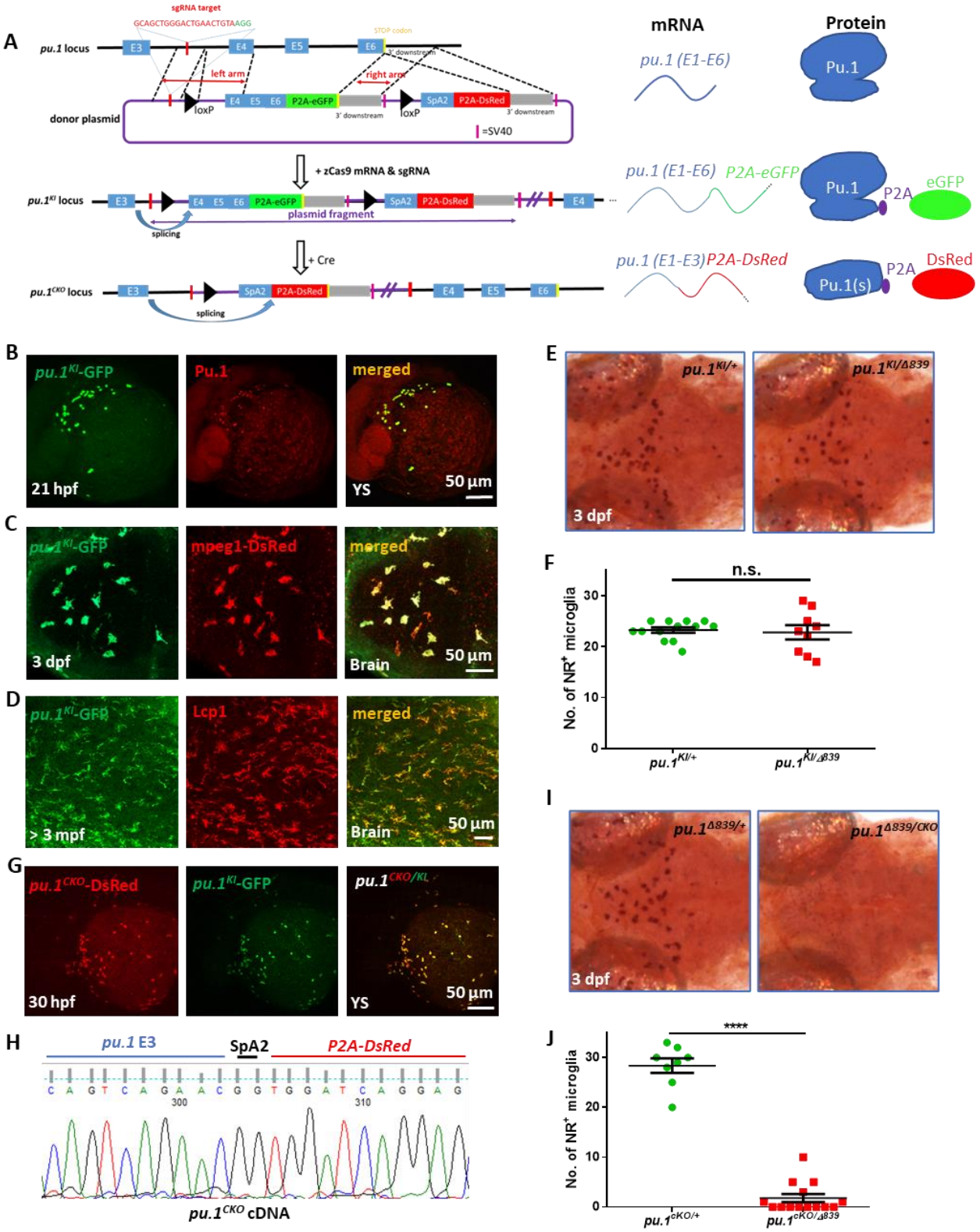
A
sgRNA target
GCAGCTGGGACTGAACTGTAAGG
STOP codon
pu.1 locus
E3
E4
E5
E6
3' downstream
left arm
right arm
donor plasmid
loxP
E4 E5 E6 P2A-eGFP
SpA2 P2A-DsRed
3' downstream
=SV40
+ zCas9 mRNA & sgRNA
pu.1KI locus
splicing
plasmid fragment
+ Cre
pu.1CKO locus
mRNA
Protein
pu.1 (E1-E6)
Pu.1
P2A-eGFP
P2A
eGFP
pu.1 (E1-E3)P2A-DsRed
Pu.1(s)
DsRed
B
pu.1KI-GFP
Pu.1
merged
21 hpf
YS
50 µm
C
mpeg1-DsRed
3 dpf
Brain
D
Lcp1
> 3 mpf
G
pu.1CKO-DsRed
pu.1KI-GFP
pu.1CKO/KI
30 hpf
H
pu.1 E3
SpA2
P2A-DsRed
C A G T C A G A A C G G T G G A T C A G G A G
300
310
pu.1CKO cDNA
E
pu.1KI/+
pu.1KI/Δ839
3 dpf
F
n.s.
No. of NR+ microglia
30
20
10
0
pu.1KI/+
pu.1KI/Δ839
I
pu.1Δ839/+
pu.1Δ839/CKO
3 dpf
J
****
No. of NR+ microglia
30
20
10
0
pu.1cKO/+
pu.1cKO/Δ839

Figure 3

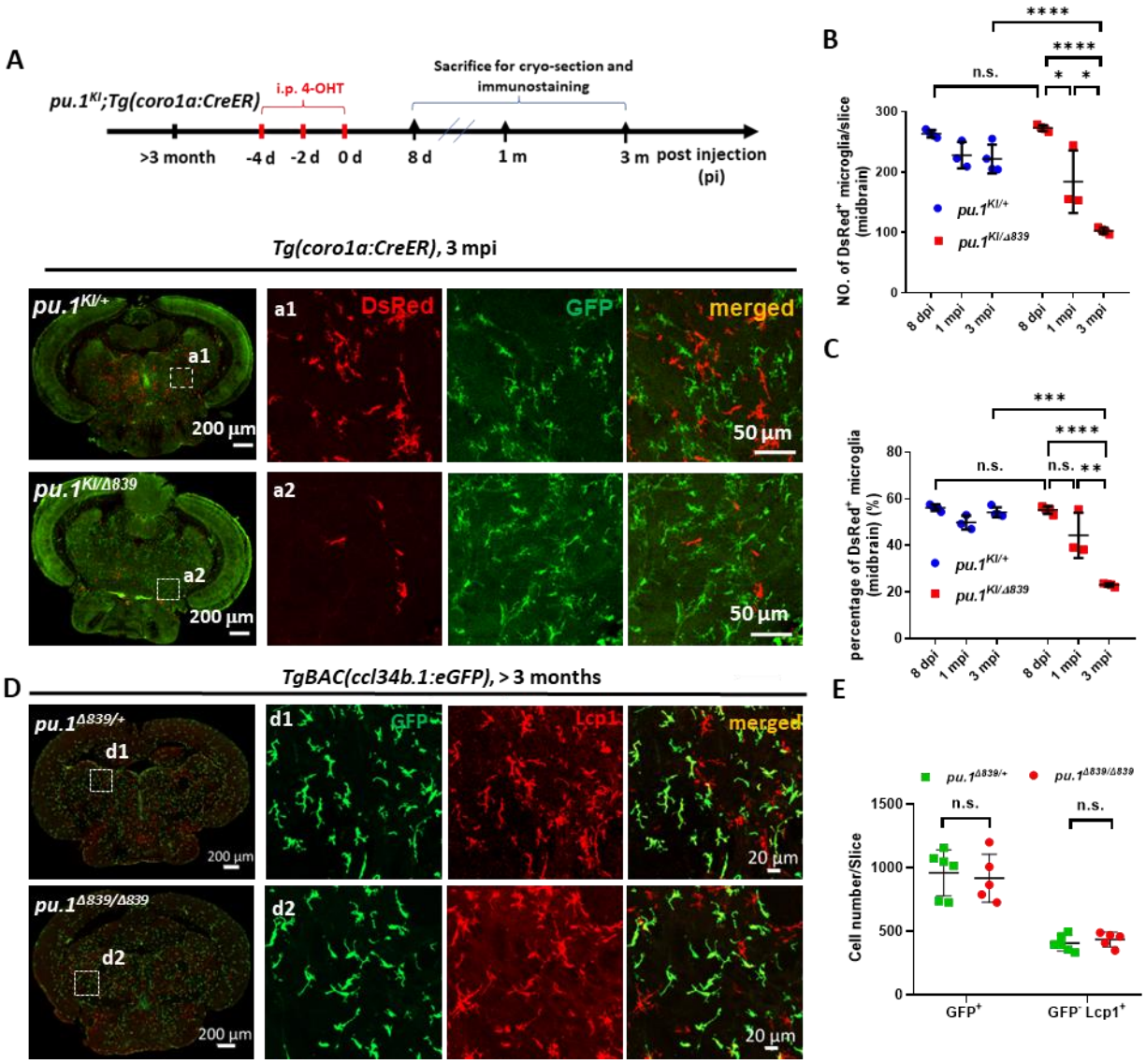
A
pu.1KI;Tg(coro1a:CreER)
i.p. 4-OHT
Sacrifice for cryo-section and immunostaining
>3 month
-4 d
-2 d
0 d
8 d
1 m
3 m
post injection (pi)
Tg(coro1a:CreER), 3 mpi
pu.1KI/+
a1
200 µm
DsRed
GFP
merged
50 µm
pu.1KI/Δ839
a2
200 µm
50 µm
B
NO. of DsRed+ microglia/slice (midbrain)
pu.1KI/+
pu.1KI/Δ839
8 dpi
1 mpi
3 mpi
n.s.
****
C
percentage of DsRed+ microglia (midbrain) (%)
***
****
n.s.
**
D
TgBAC(ccl34b.1:eGFP), > 3 months
pu.1Δ839/+
d1
200 µm
GFP
Lcp1
merged
20 µm
pu.1Δ839/Δ839
d2
E
Cell number/Slice
pu.1Δ839/+
pu.1Δ839/Δ839
GFP+
GFP- Lcp1+

Figure 4

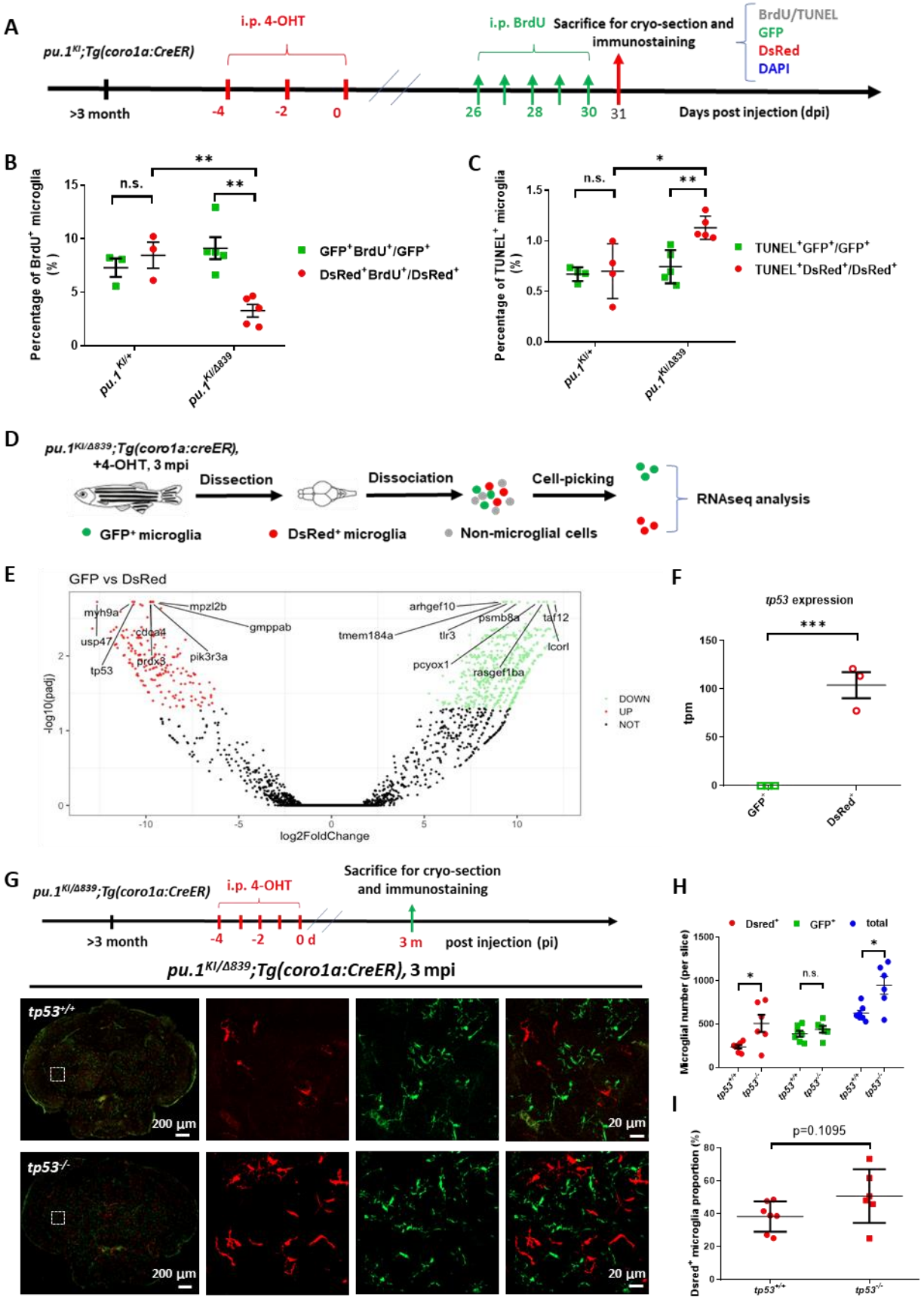
A
pu.1KI;Tg(coro1a:CreER)
i.p. 4-OHT
i.p. BrdU
Sacrifice for cryo-section and immunostaining
BrdU/TUNEL
GFP
DsRed
DAPI
>3 month
-4
-2
0
26
28
30
31
Days post injection (dpi)
B
Percentage of BrdU+ microglia (%)
n.s.
**
GFP+BrdU+/GFP+
DsRed+BrdU+/DsRed+
pu.1 KI/+
pu.1KI/Δ839
C
Percentage of TUNEL+ microglia (%)
n.s.
*
**
TUNEL+GFP+/GFP+
TUNEL+DsRed+/DsRed+
D
pu.1KI/Δ839;Tg(coro1a:creER), +4-OHT, 3 mpi
Dissection
Dissociation
Cell-picking
RNAseq analysis
GFP+ microglia
DsRed+ microglia
Non-microglial cells
E
GFP vs DsRed
myh9a
mpzl2b
gmppab
usp47
cdca4
prdx3
pik3r3a
tp53
arhgef10
psmb8a
taf12
tmem184a
tlr3
lcorl
pcyox1
rasgef1ba
DOWN
UP
NOT
-log10(padj)
log2FoldChange
F
tp53 expression
***
tpm
GFP+
DsRed+
G
pu.1KI/Δ839;Tg(coro1a:CreER)
i.p. 4-OHT
Sacrifice for cryo-section and immunostaining
>3 month
-4
-2
0 d
3 m
post injection (pi)
pu.1KI/Δ839;Tg(coro1a:CreER), 3 mpi
tp53+/+
tp53-/-
200 µm
20 µm
H
Dsred+
GFP+
total
Microglial number (per slice)
*
n.s.
*
I
p=0.1095
Dsred+ microglia proportion (%)
tp53+/+
tp53-/-

Figure 5

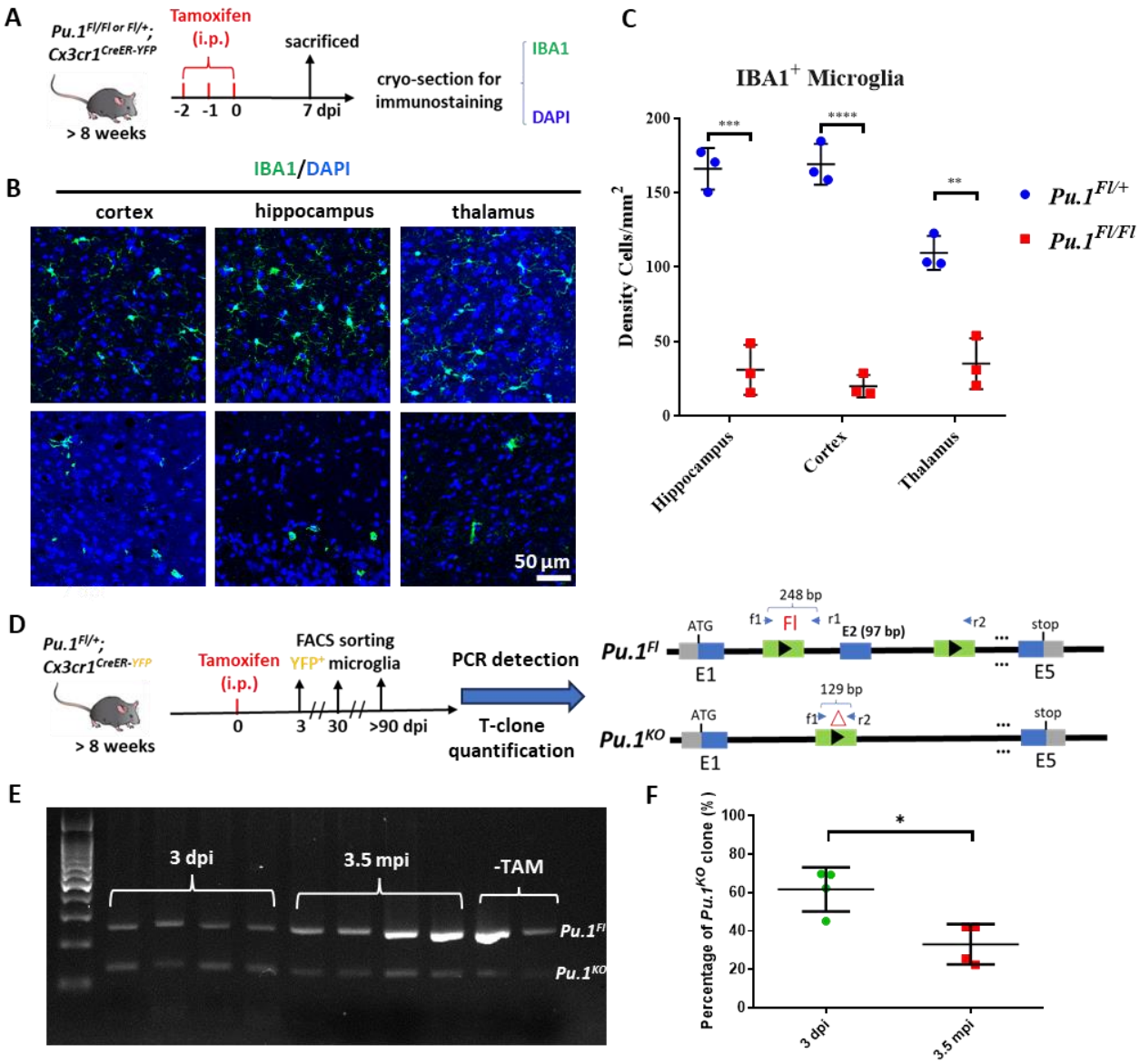
A
Pu.1Fl/Fl or Fl/+; Cx3cr1CreER-YFP
> 8 weeks
Tamoxifen (i.p.)
-2 -1 0
sacrificed
7 dpi
cryo-section for immunostaining
IBA1
DAPI
B
IBA1/DAPI
cortex
hippocampus
thalamus
50 µm
C
IBA1+ Microglia
Density Cells/mm2
200
150
100
50
0
***
****
**
Pu.1Fl/+
Pu.1Fl/Fl
Hippocampus
Cortex
Thalamus
D
Pu.1Fl/+; Cx3cr1CreER-YFP
> 8 weeks
Tamoxifen (i.p.)
FACS sorting
YFP+ microglia
0
3
30
>90 dpi
PCR detection
T-clone quantification
248 bp
ATG
f1
Fl
r1
E2 (97 bp)
r2
stop
Pu.1Fl
E1
E5
129 bp
Pu.1KO
E
3 dpi
3.5 mpi
-TAM
Pu.1Fl
Pu.1KO
F
Percentage of Pu.1KO clone (%)
100
80
60
40
20
0
*
3 dpi
3.5 mpi